

For Reference

Not to be taken from this room

ENSLAPP-A-491/94

The Gamma-ray Galactic Diffuse Radiation and Cerenkov Telescopes

P. Chardonnet^{a,b}, P. Salati^{a,b,c}, J. Silk^d, I. Grenier^e and G. Smoot^f

a) Theoretical Physics Group ENSLAPP, BP110, F-74941 Annecy-le-Vieux Cedex, France.

b) Université de Savoie, BP1104 73011 Chambéry Cedex, France.

c) Institut Universitaire de France.

d) 545, Campbell Hall, Astronomy Department, University of California at Berkeley, Berkeley CA 94720, USA.

e) Département d'Astrophysique, Centre d'Etudes Nucléaires de Saclay, F-91191 Gif-sur-Yvette Cedex, France.

f) Building 50, Room 205, Lawrence Berkeley Laboratory, 1 Cyclotron road, Berkeley CA 94720, USA.

Abstract

By using the Pythia version of the Lund Monte-Carlo, we study the photon yield of proton-proton collisions in the energy range between 10 GeV and 1 TeV.

The resulting photon spectrum turns out to scale roughly with incident energy. Then, by folding the energy spectrum of cosmic-ray protons with the distribution of HI and CO, the Galactic diffuse emission of γ -rays above 100 GeV is mapped. Prospects for observing that diffuse radiation with atmospheric Cerenkov telescopes are discussed. Present instruments are able to detect the γ -ray glow of the Galactic center. The latter will be mapped by the next generation of telescopes if their energy threshold is decreased. However, a detailed survey of the Galactic ridge will be a real challenge, even in the long term. The Milagro project seems more appropriate. Finally, we investigate the γ -ray emission from weakly interacting massive particles clustering at the Galactic center. Those species have been speculated as a major component of the halo dark matter. We show that their γ -ray signal is swamped in the Galactic diffuse radiation and cannot be observed at TeV energies.

1 - Introduction.

The diffuse γ -ray background provides a unique probe of the Galactic cosmic ray flux and the interstellar gas distribution. It is especially useful for studying the contribution to the Galactic hydrogen content of optically thick HI and cold, dense H₂. Diffuse γ -radiation has even been proposed as a probe of annihilating dark matter particles, either in the halo or concentrated in the Galactic bulge. Hitherto, observations of diffuse γ -radiation have been performed from space (SAS-2, COS-B, GRO). However it is also possible to observe diffuse Galactic γ -radiation using ground-based arrays of Cerenkov light detectors. These observations would necessarily be at higher energies than those hitherto measured, for example by GRO.

In this article we first recompute the diffuse gamma ray fluxes, paying particular attention to energies in the range between 10 GeV and 1 TeV. There is actually an energy gap between the GRO measurements ($\lesssim 30$ GeV) and the Cerenkov observations ($\gtrsim 200$ GeV). This range will soon be explored by decreasing, for instance, the energy threshold of Cerenkov telescopes. We then describe the future prospects for mapping the Galaxy at high energy, and for extracting any more exotic component to the diffuse radiation, such as the signal from annihilating halo or bulge dark matter.

Three mechanisms are responsible for the existence of the gamma ray diffuse emission of the Galaxy. First, cosmic ray nuclei undergo spallation collisions with the interstellar material. Then, electromagnetic interactions of cosmic ray electrons with the Galactic gas

lead to the production of bremsstrahlung γ -rays. Finally, ultra-high energy electrons may boost the energy of optical and infrared stellar photons through inverse Compton scattering. Above a few GeV, the first process is dominant. Section 2 is devoted to a Monte-Carlo simulation of proton-proton interactions and their photon yield, mainly through π^0 decays. The γ -ray emissivity per hydrogen atom undergoing spallation reactions with the Galactic cosmic ray nuclei is derived. The gamma ray diffuse emission of the Galaxy, above 100 GeV, is evaluated and mapped in section 3. We indicate how it may be derived for any energy in the GeV-TeV range. Prospects for detecting that Galactic diffuse radiation with atmospheric Cerenkov telescopes are discussed in section 4. Even in the long term, a few years will still be necessary to map the Galactic ridge with instruments covering several square kilometers. Detectors such as Milagro seem more appropriate. Finally, Ipser and Sikivie (1987) have advocated the possibility of a highly concentrated nucleus of neutralinos at the Galactic center. Urban *et al.* (1992) have recently claimed that the resulting annihilation γ -ray signal could be detected by Cerenkov telescopes. In section 5, we are less optimistic : this exotic emission is shown to be swamped in the diffuse Galactic emission. We conclude in section 6.

2 - High energy collisions and the γ -ray emissivity.

We have used the event generator Pythia (Bengtsson *et al.* 1987) to investigate the production of photons resulting from the collision of high-energy protons with protons

at rest. Such a process simulates the spallation reactions taking place in the Galactic gas, where cosmic-ray protons and nuclei interact with the interstellar material, mostly neutral (HI) and molecular (H₂) hydrogen. The Pythia program is based on a Monte-Carlo technique. It is extensively used by particle physicists to simulate hadronic interactions. The program takes into account the latest results obtained at high-energy colliders. We have generated 10,000 collisions for each incident proton energy E_p and obtained the photon yield and its spectrum.

Pythia incorporates a variety of processes which, in our case, may be classified in three categories. First, the non-perturbative mechanisms include the elastic and diffractive scatterings. These reactions come into play mostly at low energies, around $E_p \sim 1 - 100$ GeV, *i.e.*, for a center-of-mass energy $\sqrt{s} \sim 1 - 10$ GeV. Most of the known resonances are therefore incorporated in the Pythia program at that stage. These states are important since they may decay into pions, and eventually into photons. At higher energies, protons behave as composite objects whose constituents, the quarks and gluons, interact with each other. The usual dominant hard-QCD processes have been taken into account in the Monte-Carlo calculations. Final quarks or gluons are associated with colored flux tubes whose subsequent fragmentation and hadronisation give rise to jets. The π^0 's which they contain decay into photons. This sequence of reactions is the dominant mechanism for the production of γ -rays. Finally, prompt photon processes have also been implemented in the simulation. Photons may be directly produced by quarks or gluons, via reactions

$$q\bar{q} \text{ or } gg \rightarrow g\gamma \text{ or } \gamma\gamma \quad \text{and} \quad qg \rightarrow q\gamma \quad . \quad (1)$$

The main results of the Pythia Monte-Carlo are summarized in fig. 1a and 1b. In the first graph, the differential spectrum $dN_\gamma/d\ln E_\gamma$ is presented as a function of the photon energy. The three curves (a), (b) and (c) correspond respectively to an incident proton energy E_p of 0.1, 1 and 10 TeV. Those curves exhibit a noticeable invariance with respect to the energy scale. Each of them may be deduced from the others by a simple shift in the photon energy. In fig. 1b, the photon multiplicity $N_\gamma(> E_\gamma, E_p)$ above $E_\gamma = 10$ GeV (a), 100 GeV (b) and 1 TeV (c) is plotted against the incoming proton energy E_p . These results also are scale invariant.

An explanation of this peculiarity relies on the existence of a rapidity plateau for inclusive processes. The energy-momentum of any species produced during a collision may be completely specified in terms of the transverse mass m_\perp

$$m_\perp = \sqrt{m^2 + p_\perp^2} \quad , \quad (2)$$

of the rapidity y

$$y = \frac{1}{2} \ln \left(\frac{E + p_L}{E - p_L} \right) \quad , \quad (3)$$

and of the angular position around the beam axis, with respect to which the transverse p_\perp and longitudinal p_L components are defined. Taking advantage of this axial-symmetry and integrating out the transverse mass, the production cross section of any species may be obtained as a function of the rapidity y . In the frame where one of the initial protons is at rest, the rapidity distribution $d\sigma_\pi/dy$ of pions extends from $y = 0$ (particle at rest)

up to

$$y_{max} \simeq \ln \left(\frac{2E_p}{m_p} \right) . \quad (4)$$

It exhibits a remarkable plateau between $y \sim 2$ up to $y \sim (y_{max} - 2)$, and is symmetrical with respect to

$$y_{CM} \simeq \ln \left(\frac{\sqrt{s}}{m_p} \right) \simeq \frac{y_{max}}{2} . \quad (5)$$

Most noticeable is the invariance of the height of this plateau when the total energy \sqrt{s} in the center-of-mass frame varies. As E_p increases, the rapidity distribution spreads out to larger values of y_{max} but the magnitude of the plateau remains essentially constant. As a matter of fact, the differential spectrum of fig. 1a is the mere translation of the rapidity function for photon production

$$\frac{dN_\gamma}{d \ln E_\gamma} \propto \frac{d\sigma_\gamma}{dy} . \quad (6)$$

Therefore, if all the energies are rescaled by an overall factor of λ , the high-energy portion of that spectrum is merely shifted in rapidity by the amount $\Delta y = \ln \lambda$, hence the scale invariance exhibited by the curves. In fig.1b, the rapidity distribution has been integrated to yield the photon multiplicity $N_\gamma(> E_\gamma, E_p)$. The latter is the total number of photons above threshold E_γ , and is also a function of the incident proton energy E_p . As is clear on fig. 1b, it only depends on the ratio E_γ/E_p , *i.e.*,

$$N_\gamma(> \lambda E_\gamma, \lambda E_p) \simeq N_\gamma(> E_\gamma, E_p) . \quad (7)$$

The γ -ray emissivity per hydrogen atom has been thoroughly discussed in the literature. It is obtained from the convolution of the photon yield per proton-proton collision

with the spectrum of cosmic rays. From now on, the differential flux of protons or photons will be denoted by $\Phi(E)$ and expressed in units of $\text{cm}^{-2} \text{s}^{-1} \text{sr}^{-1} \text{GeV}^{-1}$. The integrated flux above energy E will be $\Phi(> E)$. The differential emissivity I_H , per hydrogen atom, is related to the proton-proton cross section σ_{pp} , the cosmic ray proton flux Φ_p and the differential photon yield (dN_γ/dE_γ) by

$$I_H(E_\gamma) = \int_{E_\gamma}^{+\infty} \sigma_{pp}(E_p) \left(\frac{dN_\gamma}{dE_\gamma} \right) \epsilon^M \Phi_p(E_p) dE_p \quad , \quad (8)$$

and is expressed in units of $\text{s}^{-1} \text{sr}^{-1} \text{GeV}^{-1}$. The associated integrated emissivity above threshold E_γ is defined by

$$I_H(> E_\gamma) = \int_{E_\gamma}^{+\infty} \sigma_{pp}(E_p) N_\gamma(> E_\gamma, E_p) \epsilon^M \Phi_p(E_p) dE_p \quad . \quad (9)$$

The spectrum of cosmic ray protons has been measured over a wide range of energies. Above 100 GeV, it is well described by a power law

$$\Phi_p(E) = C (1 \text{ GeV}/E)^n \quad . \quad (10)$$

Observations performed between 50 GeV and 2 TeV (Ryan *et al.* 1972) yield a magnitude of $C = 1.8 \text{ cm}^{-2} \text{s}^{-1} \text{sr}^{-1} \text{GeV}^{-1}$ and a spectral index of $n = 2.75$. Above 1 TeV and up to 200 TeV, balloon borne measurements are consistent with $C = 1.75 \text{ cm}^{-2} \text{s}^{-1} \text{sr}^{-1} \text{GeV}^{-1}$ and $n = 2.73$. The latter values have been used in our calculations, with a proton energy spectrum extending from 10 GeV up to 10^4 TeV. Note that in Bereziusky *et al.* (1993), the spectral index is also $n = 2.73$ whereas the magnitude of the total cosmic ray spectrum is assumed to be $C = 1.59 \text{ cm}^{-2} \text{s}^{-1} \text{sr}^{-1} \text{GeV}^{-1}$, slightly below our value. Finally, a global

coefficient $\epsilon^M = 1.52$ accounts for the presence of heavy nuclei both in cosmic rays and in the interstellar medium (Bialas *et al.* 1976; Gaisser and Schaefer 1992).

In fig. 2, the emissivity $I_H(E_\gamma)$ of an hydrogen atom embedded in the cosmic ray proton flux (10) is plotted against the photon energy E_γ . It decreases steeply, approximately like $E_\gamma^{-2.73}$. Actually, the total interaction cross section σ_{pp} increases slowly with energy, like a logarithm. That slow increase is directly included in the Pythia Monte-Carlo which we use. Relation (7) implies that the integrated emissivity $I_H(> E)$ scales like the cosmic ray proton flux $\Phi_p(> E)$ and varies with energy like E^{1-n} . Our emissivity (solid line) compares fairly well with the value derived by Stecker (1988)

$$I_H(E) = (3.7 \times 10^{-27} \text{ s}^{-1} \text{ sr}^{-1} \text{ GeV}^{-1}) (1 \text{ GeV}/E)^{2.86} , \quad (11)$$

which is plotted as the short dashed curve. Small differences arise from a somewhat harder cosmic ray spectrum in our case for which the index is 2.73 instead of 2.86, and from the fact that, in our calculations, violations of scale invariance are naturally incorporated in the Pythia Monte-Carlo. In both cases, only nuclear interactions of cosmic rays with matter have been taken into account. The dotted curve represents the bremsstrahlung emissivity due to cosmic ray electrons (Stecker 1988; Bertsch 1993)

$$I_H(E) = (1.7 \times 10^{-27} \text{ s}^{-1} \text{ sr}^{-1} \text{ GeV}^{-1}) (1 \text{ GeV}/E)^{3.3} . \quad (12)$$

At high energy, this component is negligible. Around 1 TeV, we obtain a differential emissivity of $\sim 2 \times 10^{-35} \text{ s}^{-1} \text{ sr}^{-1} \text{ GeV}^{-1}$ which translates into the integrated emissivity

$$I_H(> E) \simeq (1.2 \times 10^{-32} \text{ s}^{-1} \text{ sr}^{-1}) (1 \text{ TeV}/E)^{1.73} . \quad (13)$$

The conversion factor obtained by Berezhinsky *et al.* (1993) for the integral γ -ray flux above 1 TeV is $6.02 \times 10^{-11} \text{ cm}^{-2} \text{ s}^{-1} \text{ sr}^{-1}$ for an hydrogen column density of $10^{22} \text{ atom cm}^{-2}$. If the differences in the cosmic ray flux and in the global coefficient ϵ^M are taken into account, our result is only 45% larger than the emissivity calculated by Berezhinsky *et al.*. In the next section, the integrated γ -ray emissivity above 50, 100 and 200 GeV will be set equal respectively to 19.6, 6.06 and $1.83 \times (10^{-31} \text{ s}^{-1} \text{ sr}^{-1})$.

3 - The Galactic γ -ray diffuse emission between 10 GeV and 1 TeV.

The photon flux is obtained by folding the γ -ray emissivity with the total proton column density in the direction of observation

$$\Phi_\gamma = \left\{ \int dr n_H(r) I_H(r) \right\} . \quad (14)$$

We have assumed that the cosmic ray flux is homogeneous all over the Galaxy. This hypothesis is not completely correct, but is nevertheless sufficient as regards the accuracy of our estimates. As discussed by Bertsch *et al.* (1993), we should underestimate the diffuse emission from the Galactic center by at most 50%. Note however that any substantial deviation from our predictions would signal an excess or a deficiency in the local density of cosmic ray protons along the line of sight. Observations of the Galactic diffuse emission should therefore give indirect but valuable informations on the propagation of cosmic rays

inside our Galaxy. That propagation is believed to be a diffusion inside chaotic magnetic fields and is expected to depend on the energy of the particles.

In fig. 3a and 3b, the total hydrogen column density is set equal to its Galactic center average, *i.e.*, 5.0×10^{22} atom cm⁻². The first plot displays the evolution of the photon-to-proton integrated flux ratio above energy E , $\Phi_\gamma(> E)/\Phi_p(> E)$, for various values of the spectral index n of the cosmic ray emission. The magnitude C of the latter cancels out. This ratio depends moderately on the energy, for reasons mentioned in the previous section. The softer the proton spectrum, the lower the ratio. Since the integrated photon and proton spectra approximately scale with each other, the diffuse γ -ray background $\Phi_\gamma(E_\gamma)$ has the same spectral index as the cosmic ray emission from which it originates. In fig. 3b, the ratio of the integrated fluxes above 100 GeV is presented as a function of the spectral index n . The same trend as in plot 3a appears. That ratio decreases with increasing values of n .

The column density of neutral hydrogen (HI) is obtained from surveys at radio wavelengths of the Galactic 21 cm hyperfine emission (see for instance Burton 1988; Dickey and Lockman 1990). Molecular hydrogen H₂ is not detected directly. It clusters in clouds and its distribution is inferred from the tracer molecule carbon monoxide (CO). The transition between the rotation levels $J = 1 \rightarrow 0$ of the latter, detected at 2.6 mm, plays the role of the hyperfine transition for neutral hydrogen. We used the results of the Columbia survey (Dame *et al.* 1987) which maps the integrated CO intensity, expressed in K km s⁻¹, along the line of sight, in a region of the sky extending from $b = -25$ to $+25$ degrees.

The conversion factor between the CO transition intensity and the H₂ column density was taken from Strong *et al.* (1988)

$$X = \frac{N(\text{H}_2)}{W_{\text{CO}}} = 2.3 \times 10^{20} \text{ molecules cm}^{-2} / (\text{K km s}^{-1}) . \quad (15)$$

A similar result has been obtained by Bertsch *et al.* (1993) with a factor X of 2×10^{20} molecules cm⁻² / (K km s⁻¹). This calibration factor is a Galactic average value. In particular, it should not be used towards the Galactic center where very large and unusual values of the CO velocities suggest that molecular clouds may undergo significant turbulence in that region. As those clouds may be less opaque than elsewhere, the proper conversion coefficient is presumably in the range between 5×10^{19} and 10^{20} molecules cm⁻² / (K km s⁻¹) (Bhat *et al.* 1985). We therefore used a calibration factor $X \simeq 0.8 \times 10^{20}$ molecules cm⁻² / (K km s⁻¹) in the region extending over $|l| < 5$ degrees and $|b| < 2$ degrees around the Galactic center. The total proton column density is eventually derived by folding both HI and CO distributions together to get $N(\text{HI}) + 2N(\text{H}_2)$. We disregarded the ionized HII component which Bertsch *et al.* (1993) showed to be negligible.

The expected flux of γ -rays above 100 GeV is plotted in fig. 4 as a function of Galactic latitude b and longitude l . The largest value of 9.1×10^{-8} cm⁻² s⁻¹ sr⁻¹ corresponds to the equatorial region close to the Galactic center. Most of the signal is concentrated inside the disk. Note that both Galactic arms are clearly visible in the direction of Cygnus and Vela. Any value below 10^{-10} cm⁻² s⁻¹ sr⁻¹ has been suppressed for clarity. As explained previously, the flux $\Phi_\gamma(> E)$ scales with energy approximately as $E^{-1.73}$.

In order to determine the integrated photon emission above some energy E lying in the range between 10 GeV and 1 TeV, the values mapped in fig. 4 should be multiplied by a factor of $(100 \text{ GeV}/E)^{1.73}$. Remember that the color code is logarithmic so that yellow translates into a flux of $1.3 \times 10^{-9} \text{ cm}^{-2} \text{ s}^{-1} \text{ sr}^{-1}$. The differential γ -ray flux, expressed in units of $\text{cm}^{-2} \text{ s}^{-1} \text{ sr}^{-1} \text{ GeV}^{-1}$, obtains by folding our map with a multiplicative factor of $1.73 \times 10^{-2} (100 \text{ GeV}/E)^{2.73}$. In fig. 5, the photon-to-proton flux ratio

$$\phi(b, l) = \frac{\Phi_{\gamma>(> 100 \text{ GeV})}{\Phi_p(> 100 \text{ GeV})} , \quad (16)$$

is mapped as a function of Galactic coordinates b and l . As already discussed, the ratio $\phi(b, l)$ does not depend much on energy in the range between 10 GeV and 1 TeV (see fig. 3). Any value below 10^{-6} has been cut-off. The color code is also logarithmic.

4 - Prospects for detecting the Galactic γ -ray diffuse radiation at high energies.

Observation of γ -rays in the TeV range is now possible directly from the ground. When a high energy photon hits the upper atmosphere, it generates a Cerenkov shower whose associated light is directly visible by optical telescopes (Weekes 1988). The shower spreads on the Earth surface over a disk of ~ 120 m in radius, covering a surface of $\sim 45,000$ m². The shower has a smaller extension than for a proton-induced event, making it possible a priori to disentangle photons from cosmic ray nuclei. Energies can be determined with a 15 to 20% accuracy. Cerenkov detectors are undergoing significant development. They have successfully found a few point sources (Weekes *et al.* 1989; Goret *et al.* 1993; Baillon *et al.* 1993). Their effective collecting area is actually very large and could be further increased by expanding the array of ground telescopes which trace back the shower light. Such an upgrade of the existing detectors would also lower the energy threshold.

The number of γ -rays of the Galactic diffuse emission, detected by an atmospheric Cerenkov telescope (ACT) of the same calibre as Asgat (Goret *et al.* 1993), Themistocle (Baillon *et al.* 1993) or Whipple (Weekes *et al.* 1989), is a function of the effective area S of detection, of the angular aperture Ω and of the exposure time T

$$N_{\gamma}(> E) \simeq 1.26 \text{ photon} \left\{ \frac{\phi(b, l)}{10^{-5}} \right\} \left(\frac{E}{100 \text{ GeV}} \right)^{-1.73} \left(\frac{S}{10^8 \text{ cm}^2} \right) \left(\frac{T}{1 \text{ h}} \right) \left(\frac{\Omega}{10^{-3} \text{ sr}} \right) . \quad (17)$$

As the ground is illuminated by the shower around the impact point up to distances of

approximately 120 m, the effective surface of detection is much larger than the total area of the collecting mirrors. For an ACT with a set-up similar to the Granite experiment at the Whipple Observatory, S is as large as 63,000 m² when the two telescopes, each 10 m in diameter, are used independently. The angular resolution reaches down to 3×10^{-6} sr. Because high-energy photons are detected within a cone whose half-angle is ~ 1.5 degree, the angular acceptance is $\Omega \sim 2.1 \times 10^{-3}$ sr. The amount of γ -rays which such a device would collect during a one hour period time, per square degree and originating from the Galactic center region where $\phi(b, l) > 9 \times 10^{-5}$ (see fig. 5), may be expressed as

$$N_{\gamma}(> E) \gtrsim 21 \text{ photons} \left(\frac{E}{100 \text{ GeV}} \right)^{-1.73} . \quad (18)$$

It depends sensitively on the threshold energy E . In fig. 6, this number is mapped as a function of Galactic latitude and longitude, for three values of E . Most of the signal is concentrated in the Galactic disk, towards the center. The peak value corresponds to $\phi \simeq 2.59 \times 10^{-4}$. By decreasing the energy threshold of the detector, the signal considerably improves as more and more features become apparent. Above 200 GeV, the Galactic center is barely visible whereas, for a 50 GeV threshold, a significant portion of the disk shows up. Note that the angular acceptance of the Whipple ACT covers 7 square degrees, so that the maximum amount of collected photons is respectively 1400, 440 and 130 for the three maps (top to bottom). The scale is logarithmic. The orange contour, sitting at the middle of the color code, translates therefore into a number of $\sqrt{203} \simeq 14$ γ -rays.

Detecting the Galactic diffuse emission and mapping the Galactic ridge at TeV energies

turns out to be a challenge, with many experimental difficulties. First, statistics are low. There are few photons in the GeV-TeV range. This difficulty may be overturned by increasing the collecting area and expanding the array of optical telescopes. More serious is the way the signal is overwhelmed by a large number of misidentified cosmic ray protons or electrons interpreted as γ -rays. Finally, the field of view is small (typically 7 square degrees) and ACTs operate at night, without clouds and moonlight. That crucial point will prove to be a limiting factor in what follows.

A small fraction of the showers induced by cosmic ray protons are misinterpreted and recognized as electromagnetic events. For point-like sources, the Whipple ACT can make use of its two telescopes in coincidence. Stereoscopy allows for better recognition of hadrons, with a rejection factor of 10^3 . The energy measurement is also improved but the effective collecting area decreases down to 18,000 m². In the case of diffuse emission where the two mirrors are used independently, approximately 3% of hadronic cascades will be recorded as high-energy photons. Below 200 GeV, protons generate muons which may fall close to the detector. The corresponding Cerenkov emission takes the form of rings which are fairly easy to recognize, hence a better rejection efficiency with only 1% of misidentified muons. Cosmic ray electrons also initiate electromagnetic atmospheric showers in just the same way as photons do. Even if proton rejection was perfect, the background would mostly originate from events induced by cosmic-ray electrons. The flux of the latter has been measured between 30 GeV and 1 TeV (Nishimura *et al.* 1980)

$$\Phi_e(E) = (6.4 \times 10^{-2} \text{ cm}^{-2} \text{ s}^{-1} \text{ sr}^{-1} \text{ GeV}^{-1}) (1 \text{ GeV}/E)^{3.3 \pm 0.2}, \quad (19)$$

basically the energy range in which we are interested. Around 100 GeV, it contributes less than 0.3% to the total cosmic ray flux and has a harder spectrum. For point sources, difference between on and off-source measurements allows for a good rejection of the background. In the case of a diffuse emission, one relies on the isotropy of cosmic ray protons and electrons. Fluctuations of the latter from one pixel to another are merely statistical. A large number of events must therefore be accumulated before those fluctuations start to be smaller than the variations of the γ -ray diffuse emission themselves. Assuming that the noise is the square-root of the number of misidentified events, we infer a signal-to-noise ratio \mathcal{R} of

$$\mathcal{R} \simeq 0.02 \left\{ \frac{\phi(b, l)}{10^{-5}} \right\} \left(\frac{E}{100 \text{ GeV}} \right)^{-0.865} \left(\frac{S}{10^8 \text{ cm}^2} \right)^{1/2} \left(\frac{T}{1 \text{ h}} \right)^{1/2} \left(\frac{\Omega}{10^{-3} \text{ sr}} \right)^{1/2}, \quad (20)$$

when $\sim 3\%$ of cosmic ray protons make up the background. If hadron rejection is so good that electrons start to come into play, the signal-to-noise ratio becomes

$$\mathcal{R} \simeq 0.08 \left\{ \frac{\phi(b, l)}{10^{-5}} \right\} \left(\frac{E}{100 \text{ GeV}} \right)^{-0.58} \left(\frac{S}{10^8 \text{ cm}^2} \right)^{1/2} \left(\frac{T}{1 \text{ h}} \right)^{1/2} \left(\frac{\Omega}{10^{-3} \text{ sr}} \right)^{1/2}. \quad (21)$$

The pixel size is denoted by Ω while E is the threshold above which events are detected. A lot of exposure time T is required in order for the signal to emerge above the fluctuations of the background. At the 1σ detection level ($\mathcal{R} = 1$), features are barely visible whereas a 3σ observation results into a clear picture. Suppose that we want to image the Galactic ridge with a resolution reaching down one square degree. The pixel size is $\Omega = 0.305 \times 10^{-3} \text{ sr}$. We give here three illustrations of the experimental difficulties related to that measurement.

The central part of fig. 5 delineated by the yellow contour corresponds to $\phi(b, l) > 9 \times 10^{-5}$. Assuming an ACT of the Granite caliber, with the same specifications as in fig. 6 and a threshold energy $E = 200$ GeV, we infer a signal-to-noise ratio of

$$\mathcal{R} \gtrsim 0.137 \left(\frac{T}{1\text{h}} \right)^{1/2}, \quad (22)$$

in each pixel. We conclude that a minimum of 53 hours are necessary to achieve a poor 1σ detection. A good picture (3σ level) requires 480 hours of observation. Remember that a total of 100 hours of exposure time per year is already considered as excellent. Imaging the Galactic center is therefore without reach of present ACTs. However, a comparison of the γ -ray diffuse radiation from the Galactic center with the signal from a high latitude region is feasible, provided that the entire field of view is used, with $\Omega = 7$ square degrees. Only 8 hours are necessary in each direction to reach a 1σ measurement. For a 2σ observation, a total of 60 hours are necessary to detect the γ -ray glow of the Galactic center.

For the Cerenkov Array at Themis (CAT, see Degrange, B. *et al.* 1993), conditions are already met for a 200 GeV threshold whereas the long term aim is 20 to 30 GeV. The CAT experiment will have 50,000 m² of collecting area and an angular aperture of 2×10^{-3} sr. With a threshold lowered down to 20 GeV, this next generation of instruments will get a good image of the Galactic center in 11 hours, with a signal-to-noise ratio of 3 in each square degree pixel. Since the field of view is limited, mapping the region extending within $|b|$ and $|l| < 5$ degrees will require 15 exposures of different portions of the sky, resulting into a year at least of operation. That project is nevertheless feasible.

In the long term, ACT observations of the γ -ray emission from the disk will require large collecting areas. A survey at the 3σ level of the portion of fig. 5 contained inside the green-blue region ($\phi > 10^{-5}$), with one hour of exposure for each picture, translates into

$$S > (46 \text{ km}^2) \left(\frac{E}{100 \text{ GeV}} \right)^{1.16} . \quad (23)$$

Reducing the energy threshold E turns out to be of paramount importance. The future of ACTs lies in large arrays of telescopes, with mirrors used in coincidence to lower the threshold and to reject more efficiently hadron showers. In relation (23), the background is assumed to consist only of cosmic ray electrons. For a 20 GeV threshold, the detailed survey of the Galactic disk will require a surface of 7 km². Here again, the small size of each picture, with a field of view of 7 square degrees at most, is a strong factor against the use of ACTs to measure the Galactic diffuse emission. Mapping the Galactic disk at all longitudes and $|b| < 10$ degrees necessitates a thousand different pictures and several years of continuous observation.

In the case of satellite-borne devices, the background is easier to tackle. For the Gamma-Ray Large Area Silicon Telescope project (GLAST see Michelson 1993), the efficiency of proton rejection, 5×10^4 , is quite large. Particle energies are measured in the range between 20 MeV and 1 TeV. The detector covers essentially the entire sky. However, the effective area S is small, with only 10^4 cm². The number of photons collected in one live year of operation turns out to be

$$N_{\gamma}(> E) \simeq 18 \left\{ \frac{\phi(b,l)}{10^{-5}} \right\} \left(\frac{E}{10 \text{ GeV}} \right)^{-1.73} , \quad (24)$$

per square degree. Observation of the central region of our Galaxy is possible if the satellite operates for several years.

The Milagro project consists in a 5,000 m² pond operating as a water Cerenkov detector (see for instance Sinnis 1994). Milagro will be able to monitor the entire overhead sky at energies above ~ 250 GeV. It will operate night and day, rain or shine, with a high duty factor. Assuming a good rejection of the hadronic cosmic ray background, we infer a signal-to-noise ratio of

$$\mathcal{R} = 1.84 \times 10^{-2} \left(\frac{T}{1\text{h}} \right)^{1/2}, \quad (25)$$

in each square degree. Mapping the Galactic diffuse emission at the 2σ level should require $\simeq 10^4$ hours. It may be pursued as a background task. Since the angular aperture will roughly be 2π steradians, three years should be enough.

5 - The search for TeV dark matter particles.

A large portion of the mass in the universe is invisible. Its nature is still an open question. An exciting possibility is provided by the so-called weakly interacting massive particles (WIMP), *i.e.*, species with a mass between 100 GeV and a few TeV whose interactions with matter are so tenuous that gravity takes over. In the early universe, at very high temperatures, those particles were in thermal equilibrium. Later on, they decoupled from the rest of the universe because they interact weakly, and annihilated with each other. Today, their ashes may have an abundance consistent with the observed dark

matter, hence the ongoing efforts to detect them. Actually, their present mass density Ω_χ , expressed in units of the closure density, is related to their annihilation cross section $\langle \sigma_A V \rangle$

$$\Omega_\chi h^2 \simeq \frac{2.5 \times 10^{-27} \text{ cm}^3 \text{ s}^{-1}}{\langle \sigma_A V \rangle} , \quad (26)$$

where h is the Hubble constant expressed in units of $100 \text{ km s}^{-1} \text{ Mpc}^{-1}$. In supersymmetric theories, the annihilation cross section is such that the relic abundance Ω_χ may reach unity. Those dark matter particles are also believed to seed the formation of galaxies, around which they tend to concentrate. Our Galaxy is actually surrounded by a dark halo with density profile

$$\rho_\chi(r)/\rho_\chi(r_\odot) = (a^2 + r_\odot^2) / (a^2 + r^2) , \quad (27)$$

with a solar neighborhood value $\rho_\odot \simeq 0.3 \pm 0.1 \text{ GeV cm}^{-3}$. In most models, the core radius a lies in the range between 2 and 8 kpc, to be compared with the distance $r_\odot \simeq 8.5 \text{ kpc}$ of the Sun to the Galactic center. Should the Galactic dark matter be made of WIMPs, the latter would annihilate, inducing a potentially detectable signal. Annihilations of WIMPs mainly produce quark-antiquark pairs whose subsequent hadronization partly yields high-energy photons. Urban *et al.* (1992) have recently argued that if WIMPs were tightly packed at the Galactic center, observation of that region using ACT techniques would unravel their presence. These authors neglected the diffuse emission from the Galactic center, a point which we discuss now.

For haloes with a core radius $a \sim$ a few kpc, the WIMP density is so low that the gamma-ray signal is swamped in the diffuse Galactic background. However, in some

models, the dark matter density is strongly enhanced towards the Galactic center with respect to its local value. Rotation curves indicate the presence of a massive nucleus at the center of our Galaxy, with mass of $\sim 0.7 \times 10^{10} M_{\odot}$ on a scale of a few 100 pc. Dark matter could be much more concentrated in the vicinity of this central component as a result of the strong gravitational attraction of the latter. Assuming that dark matter follows an isothermal distribution, Ipser and Sikivie (1987) have shown that its density could reach extremely large values between 30 GeV cm^{-3} and 1 TeV cm^{-3} , with a typical extension of order 120 to 180 pc. Annihilations of the dark matter species would result in a strong γ -ray emission in the direction of the Galactic center, extending over a few square degrees. Note that Silk and Bloemen (1987) have pointed out that the amount of dark matter near the Galactic center is severely constrained by the COS-B satellite observations of the γ -ray flux in the energy range between 300 MeV and 5 GeV. However, no observation above 100 GeV invalidates the isothermal model of Ipser and Sikivie, provided the dark matter particles are heavy, with mass ranging from 0.1 to a few TeV.

The photon flux on Earth resulting from the dark matter annihilations taking place inside such a highly concentrated spherical region near the Galactic center may be expressed as

$$\Phi_{\gamma}^{\chi}(> E) = \frac{\langle \sigma_A V \rangle}{4\pi r_{\odot}^2} N_{\gamma}(> E) \int_{r < 150 \text{ pc}} d^3\vec{r} \{ \rho_{\chi}(r) / m_{\chi} \}^2 . \quad (28)$$

The photon multiplicity per annihilation, with energy exceeding E , is denoted by $N_{\gamma}(> E)$. Since annihilations mostly produce quark-antiquark pairs whose flavour does not affect much the photon yield (Bengtsson *et al.* 1990), $N_{\gamma}(> E)$ is fairly insensitive to

the nature of the dark matter species. Urban *et al.* (1992) found that $N_\gamma(> E)/m_\chi^2$ is approximately constant for a WIMP mass m_χ ranging from 0.4 to 4 TeV. They respectively derived a value of ~ 0.4 and 0.1 TeV^{-2} for an energy threshold E of 100 and 200 GeV. The parameter \mathcal{D} of Ipser and Sikivie (1987) is defined by

$$\int_{r < 150 \text{ pc}} d^3\vec{r} \{\rho_\chi(r)\}^2 = \frac{4\pi}{3} (150 \text{ pc})^3 \rho_0^2 \mathcal{D} , \quad (29)$$

where the mass density ρ_0 is $\sim 31 \text{ GeV cm}^{-3}$. We therefore infer a photon flux at the Earth of

$$\Phi_\gamma^\chi(> E) \simeq (1.0 \times 10^{-13} \text{ cm}^{-2} \text{ s}^{-1}) N_\gamma(> E) \left(\frac{1 \text{ TeV}}{m_\chi}\right)^2 \left(\frac{\mathcal{D}}{\Omega_\chi h^2}\right) . \quad (30)$$

An ACT similar to the Granite experiment and pointing towards the annihilating dark matter region at the Galactic center would collect

$$N_\gamma^\chi \simeq 9.5 \times 10^{-2} \text{ photons} \left(\frac{\mathcal{D}}{\Omega_\chi h^2}\right) , \quad (31)$$

per hour of observation, above 100 GeV. This signal would cover 2 to 4 square degrees and should be compared to the Galactic diffuse background of more than 21 photons per square degree as implied by relation (18). Note that the CDM annihilation signal and the Galactic diffuse emission both vary on the same angular scale of ~ 1 degree. They cannot be disentangled straightforwardly from each other. On the contrary, cosmic ray electrons and protons are fairly isotropic, hence a constant value of their contribution to the background over the entire field of view. Requiring that its annihilation signal be twice as large as the diffuse emission, we conclude that an hypothetical dark matter

nucleus at the Galactic center would become visible by ACT techniques provided that

$$\mathcal{D} > 1300 \Omega_\chi h^2 . \quad (32)$$

The largest value of $\mathcal{D} \simeq 390$ in Ipser and Sikivie (1987) translates into $\Omega_\chi h^2 < 0.3$. Therefore, if the WIMPs reach closure density, their annihilation signal is buried in the diffuse emission. As \mathcal{D} may vary between 0.3 and 390, neutralinos clustering at the Galactic center can be detected by an ACT only if they contribute very little to the astronomical missing mass. Such a situation is not plausible because WIMPs have been speculated in the first place as a major constituent of the latter. Even if such a detection was claimed, alternative explanations could account for an enhancement of the γ -ray diffuse emission at high energy. In our estimates, we used the conservative value $X = 8 \times 10^{19}$ molecules $\text{cm}^{-2} / (\text{K km s}^{-1})$ for the H_2 -CO conversion factor, a third of the Galactic average. That value has been derived from comparison between the γ -ray flux and the CO line intensity, for photon energies ranging from 300 MeV to 5 GeV. An interesting possibility suggested by Bloemen (1989) arises from the difficulty that GeV protons may have in penetrating the clouds lying in the vicinity of the Galactic center. The latter, for instance, could produce a wind which would prevent low-energy particles from approaching. A deficiency in the low-energy part of the cosmic ray spectrum would be naturally induced with respect to the local cosmic ray flux. At high energies, cosmic ray nuclei would not be affected. The correct value of X , for energies around 100 GeV, could be therefore much larger than what has been assumed in section 3, leading to an enhanced diffuse gamma ray flux towards the Galactic center. Alternatively, cosmic rays

could be anomalously enriched in heavy elements, and have a global enhancement factor ϵ^M larger than the value used here. Note that above 2 TeV per nucleon, an overabundance of cosmic ray helium by a factor of 2 has been found by comparing the observations with the low-energy extrapolations (Burnett *et al.* 1990). Such an enrichment, observed locally at high energy, could lead to a strong γ -ray emission from the Galactic center and mimic the presence of neutralinos.

6 - Conclusions.

An estimate of the γ -ray diffuse background for energies between 10 GeV and 1 TeV has been presented here. Determination of the Galactic diffuse emission at high energy is very important. First, that radiation is actually a potential background to point-like sources. Then, it provides indirect but valuable information on the propagation of cosmic rays inside our Galaxy.

We have shown that present atmospheric Cerenkov telescopes are able to detect the γ -ray glow of the Galactic center. The latter will be mapped by the next generation of instruments like CAT if their energy threshold is decreased. Because cosmic rays generate a photon emission with same spectrum, the signal-to-noise ratio considerably improves when the energy threshold is low. However, a detailed survey of the Galactic diffuse radiation will be hard to achieve with Cerenkov detectors, even with a collecting area of a few square kilometers. The short term project Milagro is more suited for mapping the

Galactic ridge, a goal which it may achieve within three years of operation.

A strong γ -ray emission from the Galactic center has been advocated as a clear signature of weakly interacting massive particles clustering and annihilating there. According to some speculations, those species are a major constituent of the astronomical dark matter. In this article, we have shown that such a γ -ray source is swamped in the Galactic diffuse radiation. Unlike Urban *et al.* (1992), we conclude that it is not likely to be detectable in the TeV energy range by atmospheric Cerenkov arrays (and by any other instrument for that matter), unless neutralinos contribute very little to the dark matter and are no longer cosmologically relevant. Even if an excess was seen, more conventional explanations could account for it.

Acknowledgements : It is a pleasure to thank Jon Aymon for assisting us with the colored plates. We acknowledge a Collaborative Research Grant from NATO under contract CRG 930695 as well as the financial support from the French Groupement de Recherche en Cosmologie. This work is supported in part by the Director, Office of Energy Research, Office of High Energy and Nuclear Physics, Division of High Energy Physics of the U.S. Department of Energy under Contract No. DE-AC03-76SF00098.

References

- Baillon, P., *et al.* 1993, *Astro-Particle Phys.*, **1**, 341.
- Bengtsson, H. U., and Sjöstrand, T. 1987, *Computer Physics Commun.*, **46**, 43.
- Bengtsson, H. U., Salati, P., and Silk, J. 1990, *Nucl. Phys. B*, **346**, 129.
- Berezinsky, V. S., Gaisser, T. K., Halzen, F., and Stanev, T. 1993, *Astro-Particle Phys.*, **1**, 281.
- Bertsch, D. L., *et al.* 1993, *Ap. J.*, **416**, 587.
- Bhat, C. L., Issa, M. R., Houston, B. P., Mayer, C. J., and Wolfendale, A. W. 1985, *Nature*, **314**, 511.
- Bialas, A., Bleszynski, M., and Czyz, W. 1976, *Nucl. Phys.*, **B111**, 461.
- Bloemen, H. 1989, *ARA&A*, **27**, 469.
- Burnett, T. H., *et al.* 1990, *Ap. J.*, **349**, L25.
- Burton, W. B. 1988, in *Galactic and Extragalactic Radio Astronomy*, 2nd ed., ed. G. L. Verschuur and K. Kellermann (New York: Springer), 295.
- Dame, T. M., *et al.* 1987, *Ap. J.*, **322**, 706.
- Degrange, B., *et al.* 1993, *Cherenkov Array at Thémis*, CAT report, ed. Imprimerie de l'Ecole polytechnique, Palaiseau, France.
- Dermer, C. D. 1986, *Astron. Astrophys.*, **157**, 223.
- Dickey, J. M., and Lockman, F. J. 1990 *ARA&A*, **28**, 215.

- Gaisser, T. K., and Schaefer, R. K. 1992, *Ap. J.*, **394**, 174.
- Goret, P., *et al.* 1993, *Astron. Astrophys.*, **270**, 401.
- Ipsier, J. R., and Sikivie, P. 1987, *Phys. Rev. D*, **35**, 3695.
- Michelson, P. F. 1993, Development of A Broadband High Energy Gamma-Ray Telescope Using Silicon Strip Detectors, GLAST proposal.
- Nishimura, J., *et al.* 1980, *Ap. J.*, **238**, 394.
- Silk, J., and Bloemen, H. 1987, *Ap. J.*, **313**, L47.
- Simmis, G. 1994, Contribution at the Conference *Trends in Astroparticle Physics*, September 22-25 1994, Stockholm, Sweden.
- Stecker, F. W. 1973, *Ap. J.*, **185**, 499.
- Stecker, F. W. 1988, in *Cosmic Gamma Rays, Neutrinos and Related Astrophysics*, ed M. M. Shapiro & J. P. Wefel (Dordrecht: Reidel) 85.
- Strong, A. W., *et al.* 1988, *Astron. Astrophys.*, **207**, 1.
- Urban, M., *et al.* 1992, *Phys. Letters B*, **293**, 149.
- Vacanti, G., *et al.* 1991, *Ap. J.*, **377**, 401.
- Weekes, T. C. 1988, *Phys. Rep.*, **160**, 1.
- Weekes, T. C., *et al.* 1989, *Ap. J.*, **342**, 379.

Figure Captions

Fig 1a : The Pythia version of the Lund Monte-Carlo has been used to simulate collisions between incoming protons and protons at rest. Such hadronic interactions produce π^0 mesons which eventually yield high-energy photons. The γ -ray differential energy spectrum $dN_\gamma/d\ln E_\gamma$ is presented as a function of the photon energy E_γ , for three values of the incident proton energy : $E_p = 100$ GeV (a), 1 TeV (b) and 10 TeV (c).

Fig 1b : The γ -ray multiplicity $N_\gamma(> E_\gamma, E_p)$ above the photon energy threshold $E_\gamma = 10$ GeV (a), 100 GeV (b) and 1 TeV (c) is plotted as a function of the incoming proton energy E_p .

Fig 2 : Hydrogen atoms, immersed in a radiation of cosmic ray nuclei with which they interact, produce γ -rays. The differential emissivity $I_H(E_\gamma)$, per atom, is expressed here in units of $10^{-30} \text{ s}^{-1} \text{ sr}^{-1} \text{ GeV}^{-1}$ and plotted against the photon energy E_γ (solid line). The short dash curve corresponds to the calculations by Stecker (1988). Both results take only into account nuclear interactions of cosmic ray nuclei on the interstellar material. The dotted curve stands for the Bremsstrahlung emissivity which is negligible.

Fig 3a : The photon-to-proton integrated flux ratio, $\Phi_\gamma(> E)/\Phi_p(> E)$, does not vary much with respect to the energy threshold E . At high energy, hadronic interactions are approximately scale invariant. Four different values for the spectral index n of the differential cosmic-ray spectrum $\Phi_p(E)$ have been presented. The total hydrogen column density corresponds to the Galactic center average value, *i.e.*, $5. \times 10^{22} \text{ atom cm}^{-2}$.

Fig 3b : The photon-to-proton integrated flux ratio above 100 GeV is featured as a function of the spectral index n . The total hydrogen column density has the same value as in fig. 3a. The softer the proton spectrum $\Phi_p(E)$, the larger the index n , and the lower the ratio $\Phi_\gamma(> 100 \text{ GeV})/\Phi_p(> 100 \text{ GeV})$.

Fig 4 : The diffuse emission of γ -rays with energy larger than 100 GeV is plotted as a function of Galactic latitude and longitude. Any value below $10^{-10} \text{ cm}^{-2} \text{ s}^{-1} \text{ sr}^{-1}$ has been suppressed. The entire sky has been projected on the oval. The center of the map corresponds to the Galactic center. The grey bands are the polar regions. The extreme left and right points both refer to the Galactic anti-center. The integrated flux $\Phi_\gamma(> E)$ scales with energy as $E^{-1.73}$. The color code is logarithmic, so that yellow corresponds to $1.3 \times 10^{-9} \text{ cm}^{-2} \text{ s}^{-1} \text{ sr}^{-1}$.

Fig 5 : The ratio $\Phi_\gamma(> 100 \text{ GeV})/\Phi_p(> 100 \text{ GeV})$ is mapped in Galactic coordinates. As discussed in section 2, it varies little with energy. Any value below 10^{-6} has been cut-off. The color code is logarithmic. The region delineated by the yellow contour corresponds to a ratio larger than 9×10^{-5} and a fairly strong diffuse emission.

Fig 6 : The number of high-energy photons which a Whipple-like telescope could collect, within one hour, per square degree, is mapped in Galactic coordinates. The effective area of detection is $63,000 \text{ m}^2$. The photon energy threshold has been respectively set equal to 50, 100 and 200 GeV for the three maps. Note that the angular acceptance of the telescope corresponds to 7 square degrees. The logarithmic color code is the same for the three plots.

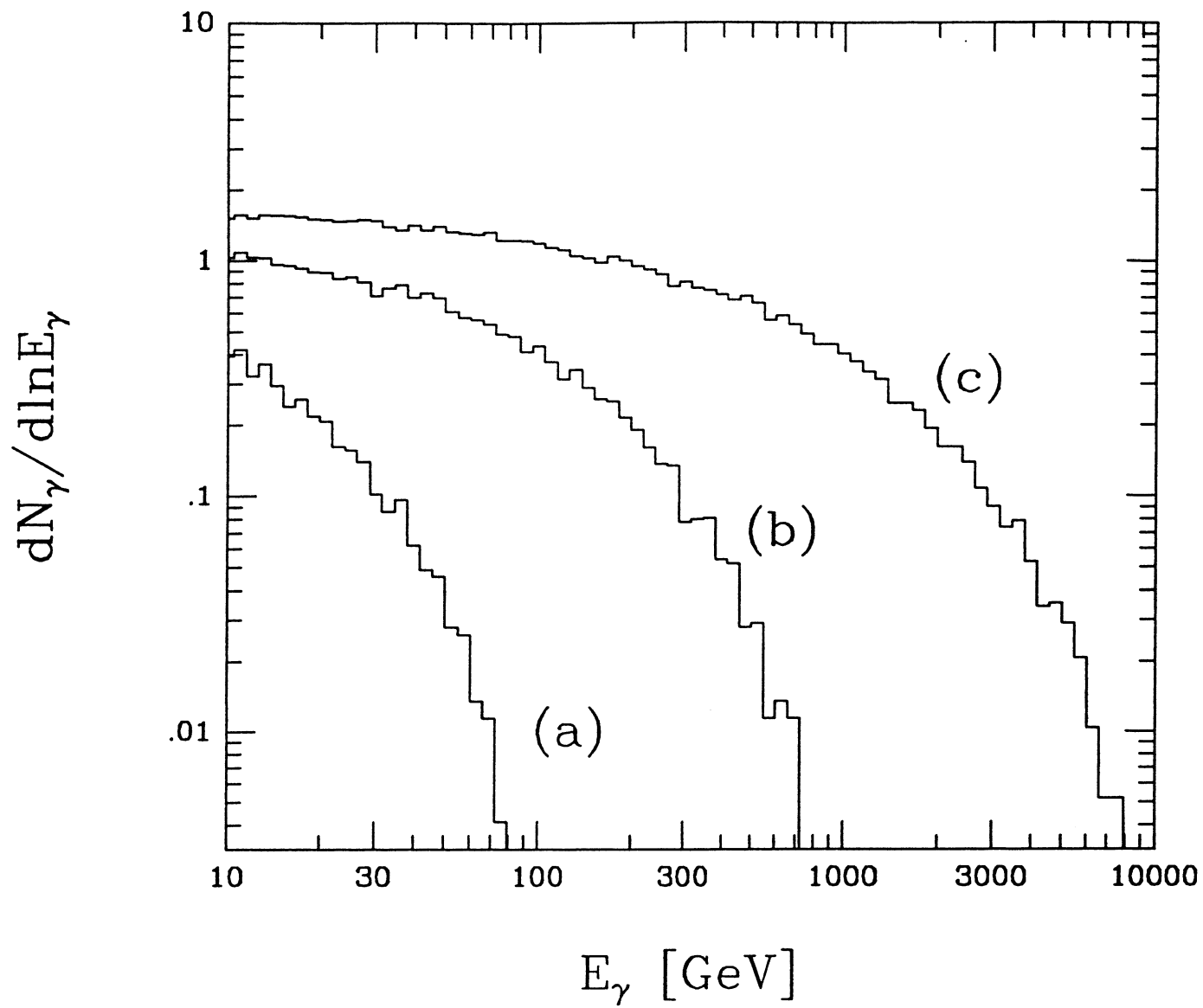


Fig 1a

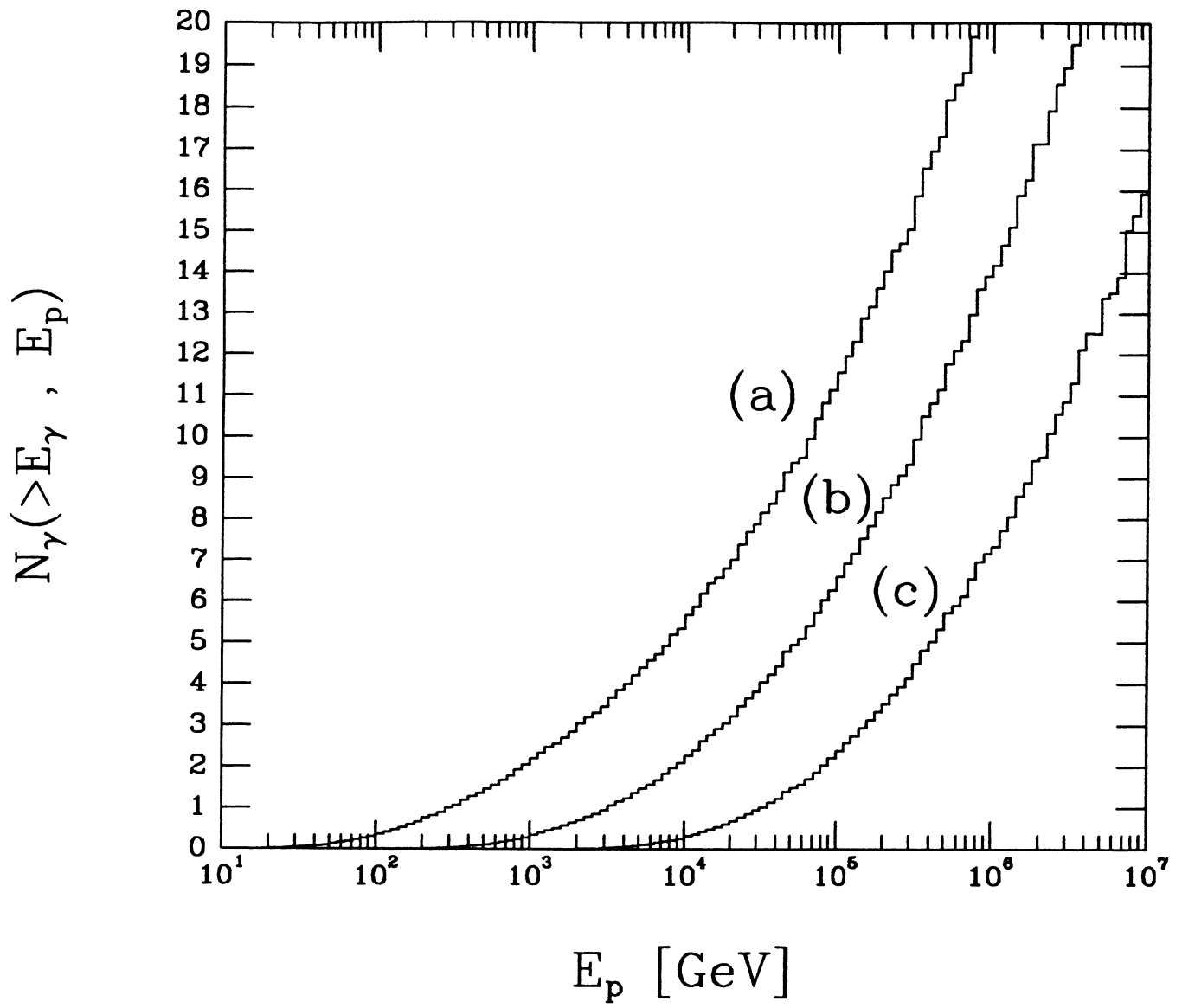


Fig 1b

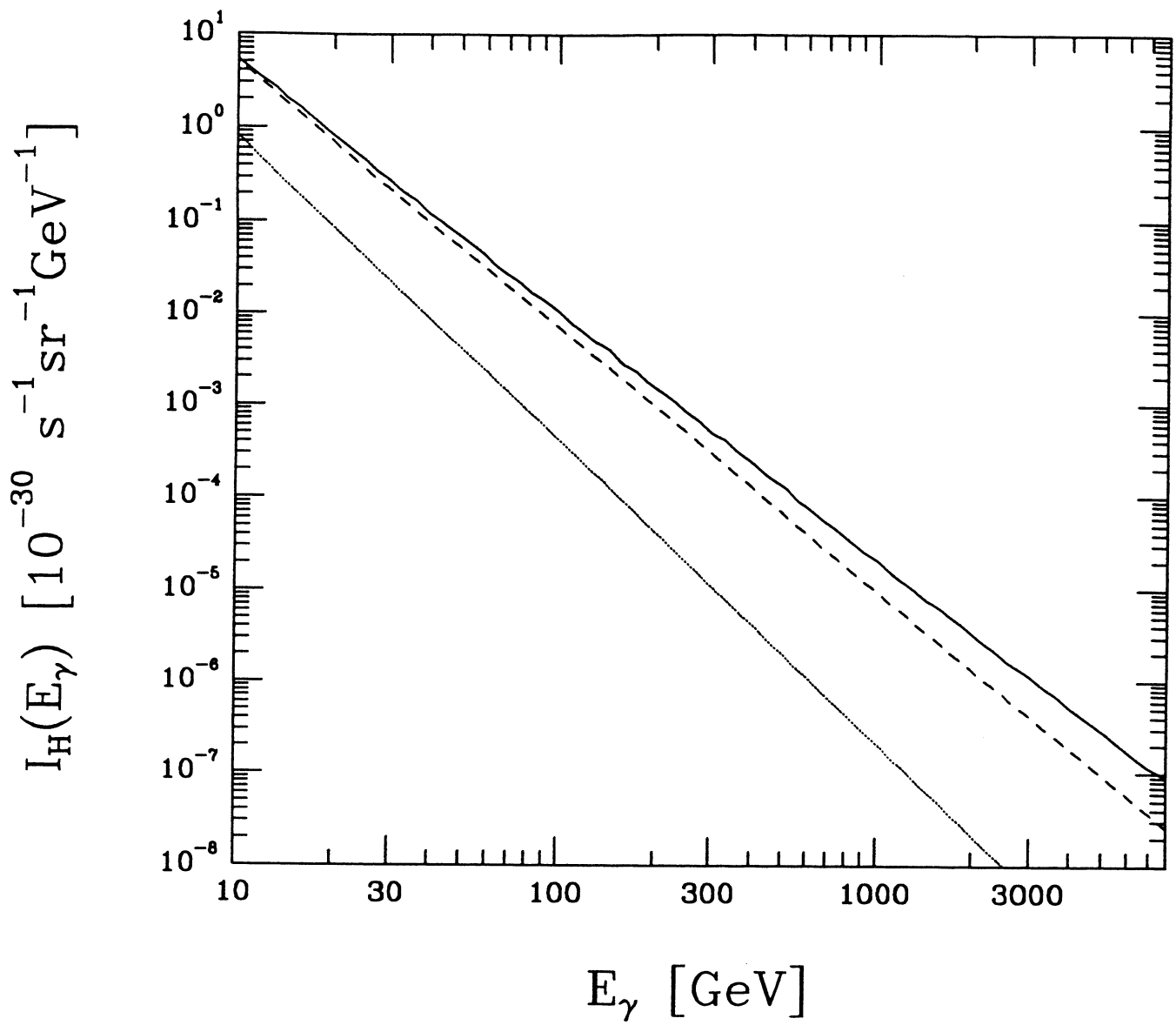


Fig 2

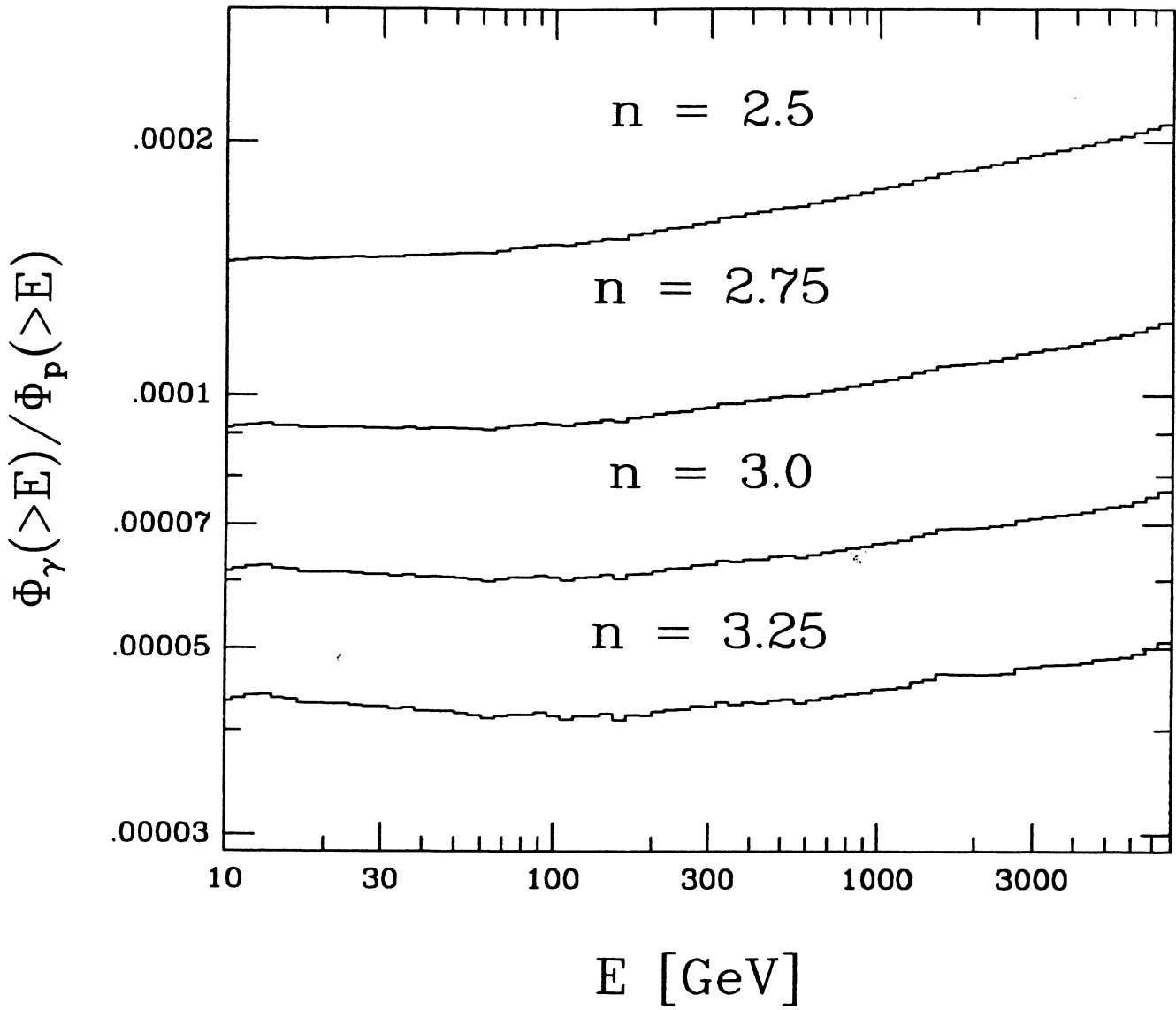


Fig 3a

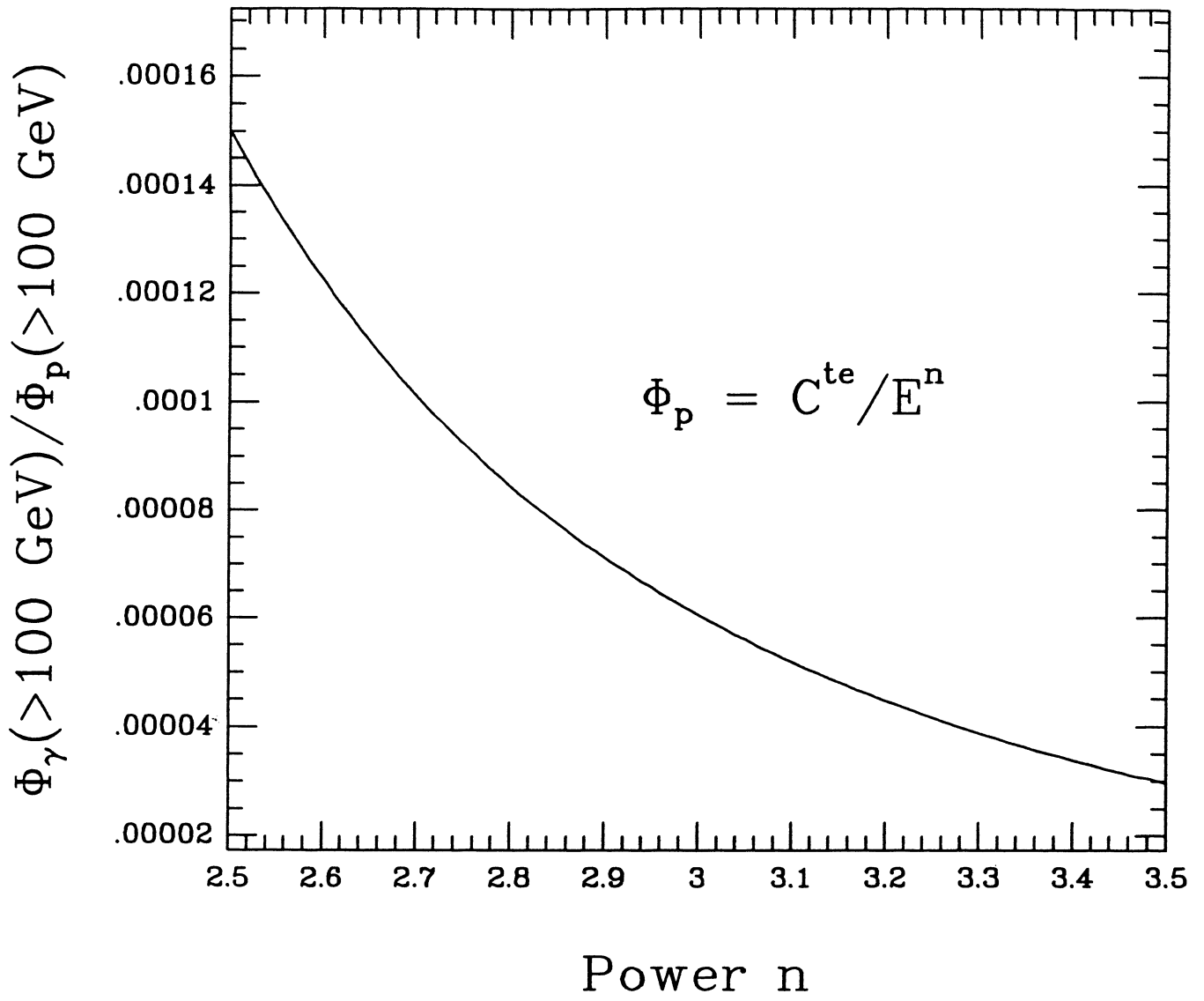


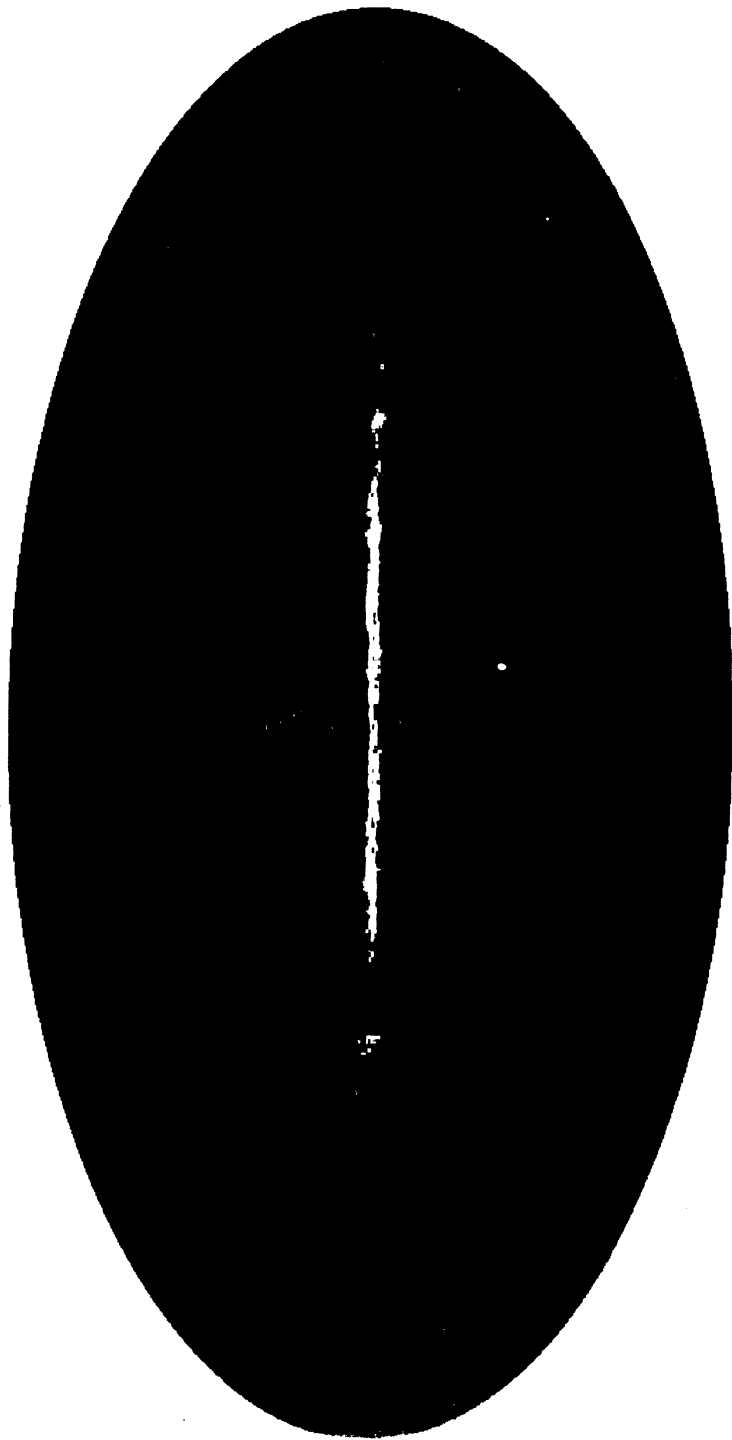
Fig 3b

Figure 4



1.0E-10 ■ ■ ■ 9.1E-8

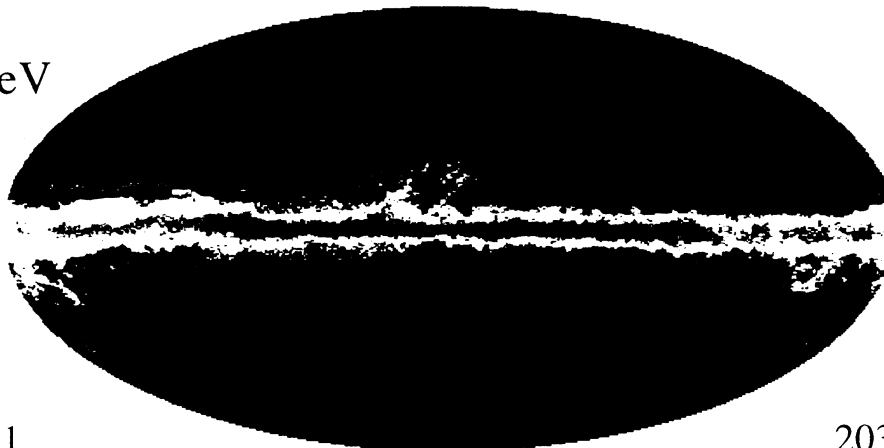
Figure 5



1.0E-6 ■ 2.59E-4

Figure 6

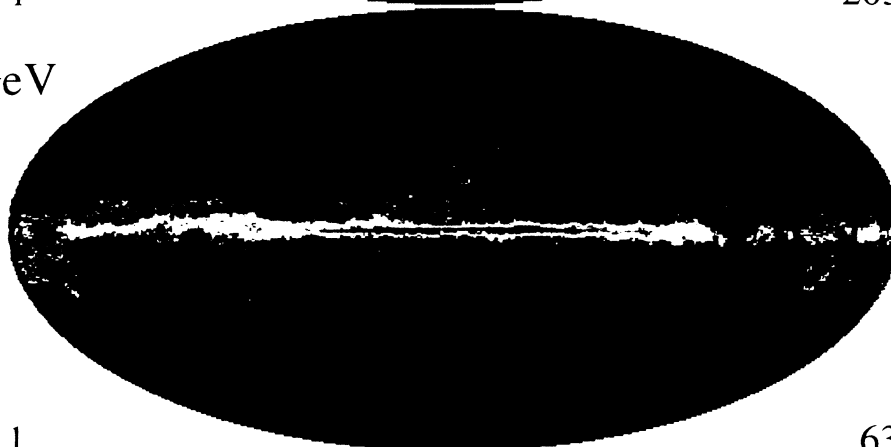
50 GeV



1

203

100 GeV



1

63

200 GeV



1

19

1 ■ ■ ■ 203